PROTEINS: Structure, Function, and Genetics 50:192–206 (2003)

Phage-Display and Correlated Mutations Identify an Essential Region of Subdomain 1C Involved in Homodimerization of *Escherichia coli* FtsA

Daniele Carettoni,[1]* Paulino Gómez-Puertas,[2] Lucía Yim,[1] Jesús Mingorance,[2] Orietta Massidda,[1] Miguel Vicente,[2] Alfonso Valencia,[2] Enrico Domenici,[1] and Daniela Anderluzzi[1]

[1]*GlaxoSmithKline Medicines Research Center, Via Fleming 4, 37135 Verona, Italy*

[2]*Centro Nacional de Biotecnología, Consejo Superior de Investigaciones Científicas, Campus Universidad Autónoma de Cantoblanco, 28049 Madrid, Spain*

ABSTRACT **FtsA plays an essential role in *Escherichia coli* cell division and is nearly ubiquitous in eubacteria. Several evidences postulated the ability of FtsA to interact with other septation proteins and with itself. To investigate these binding properties, we screened a phage-display library with FtsA. The isolated peptides defined a degenerate consensus sequence, which in turn displayed a striking similarity with residues 126–133 of FtsA itself. This result suggested that residues 126–133 were involved in homodimerization of FtsA. The hypothesis was supported by the analysis of correlated mutations, which identified a mutual relationship between a group of amino acids encompassing the ATP-binding site and a set of residues immediately downstream to amino acids 126–133. This information was used to assemble a model of a FtsA homodimer, whose accuracy was confirmed by probing multiple alternative docking solutions. Moreover, a prediction of residues responsible for protein-protein interaction validated the proposed model and confirmed once more the importance of residues 126–133 for homodimerization. To functionally characterize this region, we introduced a deletion in *ftsA*, where residues 126–133 were skipped. This mutant failed to complement conditional lethal alleles of *ftsA*, demonstrating that amino acids 126–133 play an essential role in *E. coli*. Proteins 2003;50:192–206.** © 2002 Wiley-Liss, Inc.

Key words: bacterial cell division; FtsA; homodimerization; phage-display library; correlated mutation analysis, protein-protein interaction

INTRODUCTION

Bacterial cell division is a complex process, which requires the spatially and temporally coordinated recruitment of different proteins at the division site. A pioneering genetic approach discovered the key components of the septation machinery, leading to the identification of filamentous temperature-sensitive (*fts*) mutants.[1] Many *fts* genes are clustered on the chromosome and the corresponding proteins have an essential role in initiating and progressing cell division.[2] The first detectable event of cell division is the localization of FtsZ at mid-cell to create a ring-shaped structure, named Z-ring.[3] Immediately after Z-ring assembly, FtsA is recruited at the division site.[4] The assembly of subsequent cell division proteins is strictly dependent on the presence of both FtsA and FtsZ.[3] FtsA is a 45-kDa protein highly conserved in eubacteria, which localizes at the division site in a FtsZ-dependent manner forming in its turn a ring structure at mid-cell.[4] FtsA is expressed at a very low level and post-translational modifications seem to regulate its cytosolic or membrane localization, although its precise relationships with the other proteins of the septator are still uncertain.[5,6] Many functional, genetic, and biochemical evidences indicate that FtsA directly binds FtsZ and phenotypic analysis of conditional-lethal mutants suggests that also FtsI, FtsL, FtsQ, FtsN, FtsK, and MinCD interact with FtsA, even though these latter studies did not clarify whether these contacts occur directly or indirectly.[4,7–15] On the other hand, it has been postulated that FtsA can form homodimers and perhaps polymers. The assembly of a FtsA-ring is suggestive of the formation of a multiproteic higher-order structure.[4] Furthermore, the conditionally functional allele *ftsA104* can effectively complement the temperature-sensitive mutants *ftsA2* and *ftsA3*, but inefficiently substitutes for the amber mutant *ftsA16*.[6] Finally, the C-terminus of FtsA was found to be essential for self-

Abbreviations: BSA, bovine serum albumin; MBP, maltose binding protein; NP 40, Nonidet P40; PEG, polyethylene glycol; HRP, horseradish peroxidase; TMB, 3,3′,5,5′-tetramethylbenzidine.

Grant sponsor: European Commission (DGXII) Biotechnology Program; Grant number: Cell Factory Contract No. CT96-0122.

Daniele Carettoni and Paulino Gómez-Puertas contributed equally to this work.

L. Yim's present address is Departamento de Genetica Molecular, Instituto de Investigaciones Citologicas, c/Amadeo de Saboya 4, 46010 Valencia, Spain.

O. Massidda's present address is Dipartimento di Scienze Chirurgiche, Sezione di Microbiologia, Via Palabanda 14, 09124 Cagliari, Italy.

*Correspondence to: Daniele Carettoni, Axxam Research, S. Raffaele Biomedical Science Park, Via Olgettina 58, 20132 Milano, Italy. E-mail: daniele.carettoni.dc@axxam.com

Received 10 December 2001; Accepted 15 April 2002

interaction and recent studies on FtsA from *Bacillus subtilis* confirmed its ability to form homodimers.[16,17]

Characterization of cell division proteins was recently boosted by structural studies, which demonstrated that FtsA and FtsZ share overall topological similarities with the eukaryotic cytoskeletal proteins actin and tubulin, respectively.[18,19] Whereas FtsZ is the structural and functional homologue of tubulin in bacteria,[20] FtsA was predicted to belong to the actin/hsc70/sugar kinase superfamily on the basis of the presence of the actin-fold, a conserved five-motif structure responsible for ATP-binding.[21] Biochemical and genetic studies demonstrated the ATP-binding activity of FtsA and the essentiality of those residues predicted to contact ATP.[6,17] Recently, the crystal structure of FtsA from *Thermotoga maritima* has been solved, confirming that FtsA has the same core domains and active site of the actin superfamily.[19] The most important difference between FtsA and the other members of the family is the orientation of the second subdomain (1C), which protrudes on the opposite direction with respect to actin. The remarkable structural analogies of these key components of bacterial cell division with two proteins that play a pivotal role in eukaryotic cytokinesis prompt the hypothesis that FtsZ and FtsA coordinately act to accomplish constriction at the bacterial division site.

We chose to investigate the binding features of FtsA using affinity screening of a peptide library displayed on the surface of M13 bacteriophages. This powerful technique has been widely applied to develop receptor-specific ligands, drug-delivery systems, and enzyme inhibitors and substrates.[22,23] Concerning FtsA, the identification of specific peptide ligands appeared attractive both to shed light on its poorly defined binding specificity and to explore their use as templates to discover novel antimicrobial lead compounds with broad spectrum activity. Here we report the results of molecular, functional and combinatorial approaches that converge to identify a self-interacting interface of FtsA on subdomain 1C. On the basis of these data, we propose a model for the homodimerization of FtsA, which is supported by probing multiple alternative docking solutions, by previous genetic evidences, and by a striking similarity with contacts occurring in actin homopolymers.

MATERIALS AND METHODS

Strains, Vectors, and Sequences

E. coli strains. DH5α [F^- *supE44 hsdR17 recA1 gyrA96 relA1 endA1 thi-1* Δ*lacU169(F80 lacZ*Δ*M15)*λ^-]: plasmid propagation and *ftsA*Δ*7* characterization. XL10GoldKan [Δ*(mcrA)183* Δ*(mcrCB-hsdSMR-mrr)173 endA1 supE44 thi-1 recA1 gyrA96 relA1 lacHte (F' proAB lacI*^{q}*Z*Δ*M15 Tn10 Tet*^{R} *Tn5 Kan*^{R} *Amy)*; Stratagene]: *ftsA*Δ*7* characterization. ER2537 [*F' lacI*^{q} Δ*(lacZ)M15 proA*$^+$*B*$^+$*/fhuA2 supE* Δ*(lacproAB) thi* Δ*(hsdMS-mcrB)5* (r_k m_k *mcrBC*$^-$) λ^-; New England Biolabs]: bacteriophage growth. Strains D2 [F^- *ilv thyA (deo) his ara (Am) lac125 (Am) galE trp (Am) tsx (Am) tyrT (supFA81 Ts) ftsA2*][24] and OV16 [F^- *leu ilv thyA (deo) his ara (Am) lac125 (Am) galE trp (Am) tsx (Am) tyrT (supFA81 Ts) ftsA16 (Am)*[25]]: complementation studies.

M13 bacteriophages: VCSM13 (Stratagene) and Ph.D.-7 library (New England Biolabs).

Vectors: pET28a(+) (Novagen): cloning of polyhistidine tagged FtsA (pMFV12); pBAD24: functional studies with wild-type FtsA and FtsAΔ7.[26]

Accession numbers. Orthologous FtsA sequences: *E. coli* P06137 (SwissProtein, SP); *B. aphidicola* P57309 (SP); *H. influenzae* P45068 (SP); *P. putida* AAB90170 (Genbank, G); *P. aeruginosa* P47203 (SP); *N. meningitidis* E81201 (Protein Information Resource, PIR); *B. burgdorferi* Q44774 (SP); *T. pallidum* AAC65373 (G); *D. radiodurans* D75494 (PIR); *H. pylori* Q9ZKM3 (SP); *C. jejuni* B81340 (PIR); *T. maritima* AAD36352 (G); *B. subtilis* P28264 (SP); *S. aureus* O07325 (SP); *S. pneumoniae* AAC95439 (G); *E. faecalis* O07111 (SP); *E. hirae* O07672 (SP); *S. meliloti* O30994 (SP); *A. tumefaciens* O30991 (SP); *A. aeolicus* D70347 (PIR). FtsA sequences from *Y. pestis*, *A. actinomycetemcomitans*, *N. gonorrhoeae*, *S. pyogenes,* and *C. acetobutylicum* were obtained from the NCBI Unfinished Microbial Genomes Blast Database server (http://www.ncbi.nlm.nih.gov/Microb_blast/unfinishedgenome.html) with the following accession codes:

gnl|Sanger_632|Y. pestis_Yersinia,
gnl|OUACGT_714|A. actin_Contig201,
gnl|OUACGT_485|Ngon_Contig1,
gnl|OUACGT_1315|Spyogenes_Contig1,
gnl|GTC|C.aceto_gnl,

respectively. Accession number of the FtsA structure from *T. maritima*: 1e4f (Protein Data Bank). *E. coli* MurC P17952 (SP).

Phage Panning

N-terminal histidine-tagged *E. coli* FtsA was expressed and purified as described by Yim et al.[16] Ph.D.-7 library (2×10^{13} pfu/mL, complexity 2×10^9) was screened according to the manufacturer's instructions. The first screening was carried out in TBS (50 mM Tris-HCl, 150 mM NaCl, pH 8.0), and the second in PB (50 mM Tris-HCl, 50 mM NaCl, pH 8.0). Briefly, 4 μg of his-FtsA, 0.1% BSA (Sigma) were incubated o.n. at 4°C on Ni-NTA strips (Qiagen). Strips were washed four times and then saturated with 1% BSA for 1 h at room temperature. After four washes, 2×10^{11} pfu of Ph.D.-7 library (or VCSM13) were incubated for 2 h in the presence of 0.1% BSA. Then strips were washed quickly six times, one time for 10 min and quickly again six times with the indicated amount of detergent. Bacteriophages were eluted with 0.1% BSA, 0.2 M glycin-HCl, pH 2.2, and immediately neutralized with 1:10 (v:v) 2 M Tris-base at 4°C. Eluted phages (10 μL) were titered as described by Kay et al.[27] and the remaining part was amplified by infecting 20 mL of *E. coli* ER2537 grown for 4.5 additional hours. Phages were separated by centrifugation and precipitated o.n. at 4°C by adding 1:6 (v:v) 20% PEG-8000, 2.5 M NaCl (PEG/NaCl). Phages were collected by centrifugation, washed with TBS, precipitated again with PEG/NaCl, and finally resuspended in TBS. Bacteriophages were titered and challenged by ELISA

with his-FtsA to verify the enrichment for specific binders, while 2×10^{11} pfu were used for the subsequent round. At the end of the panning procedures, phages were picked from nonconfluent plaques and individually amplified as described above. Single-strand DNA was extracted by resuspending the bacteriophage pellet in 10 mM Tris-HCl, 1 mM EDTA, 4 M NaI, pH 8.0, followed by ethanol precipitation and sequenced with −96gIII primer (New England Biolabs) using an ABI Prism 377 DNA Sequencer and BigDye Terminators Cycle Sequencing Ready Reaction Kit with Amplitaq FS DNA Polymerase (Perkin Elmer-Applied Biosystems).

ELISA

The experiment was carried out as described by Harlow and Lane.[28] Briefly, 100 μg/mL of his-FtsA, his-MurC or 1% BSA were adsorbed o.n. at 4°C on Ni-NTA strips in TBS. After four washes with TBS, strips were saturated for 1 h with 1% BSA and, after a brief wash with TBS, 1×10^9 pfu/well of bacteriophages were incubated for 1 h at room temperature. Wells were washed six times quickly, one time for 10 min and quickly again six times with TBS, 0.5% Tween 20. Rabbit polyclonal antibodies anti-fd (1:2500; Sigma) in TBS, 0.5% Tween 20 were incubated for 1 h and then washed three times with TBS, 0.5% Tween 20. HRP-labeled secondary antibodies (1:5000; Boehringer) in TBS, 0.5% Tween 20 were added for 30 min, and excess was removed with three washes in the same buffer conditions. Strips were developed by adding 100 μL of TMB (Biorad), following kinetically the reaction for 20 min in a Spectra Max 250 spectrophotometer (Molecular Devices) at OD_{370nm}. Finally 50 μL of 1 M H_2SO_4 was added, and strips were read at OD_{450nm}.

Bioinformatic Analysis

Conversion of amino acids of the peptide sequence was performed with SIMPLIFY program (GCG) by changing the local data file with physico-chemical code proposed by Taylor.[29] Multiple sequence alignment was performed with CLUSTALW.[30] Similarity between T8A-11 and FtsA was established by using BLASTP program on *E. coli* genomic CDS translations.[31]

Correlated mutation analysis was performed with program PLOTCORR.[32] Generation of 5×10^3 different docking solutions for the homodimerization model of FtsA was achieved with program GRAMM.[33]

Correlated mutation-corrected distance factor (*cd*) for each individual docking solution was calculated using the formula:[34]

$$cd = \frac{\sum_{i=1}^{i=n} d_i \cdot r_i}{n}$$

where d_i is the distance between each pair of residues, r_i is the correlation coefficient calculated by the PLOTCORR program to each pair of positions, and n is the number of correlated pairs.

Harmonic average factor (*Xd*) was calculated for each of the 5×10^3 docking solutions by the formula[34]:

$$Xd = \sum_{j=1}^{j=n} \frac{P_{jc} - P_{ja}}{d_j \cdot n}$$

where n is the number of distance bins, d_j is the upper limit for each bin, P_{jc} is the percentage of correlated pairs with distances between j and $j - 1$, and P_{ja} is the same percentage for all pairs of positions.

The neural network applied to predict protein-protein interaction residues was essentially similar to the system described by Zhou and Shan and was published elsewhere.[35,36] The neural network was trained with the set of dimer-forming pairs of known interacting proteins collected from the SPIN database (http://trantor.bioc.columbia.edu/cgi-bin/SPIN), which contains all protein interfaces obtained from Protein Data Bank. Together with these structural data, the network used as input also the evolutive information stored in multiple sequence alignments from the HSSP database (http://www.cmbi.kun.nl/swift/hssp/). The validation phase of the network was based on the analysis of known dimers in a threefold cross-validation procedure and showed an accuracy value of 72% for residues correctly detected as amino acids involved in protein interaction over the whole data set. This result is comparable to the 70% value obtained by Zhou and Shan,[35] thus supporting the reliability of the system.

Functional Analysis of FtsAΔ7

ftsAΔ7 was cloned in pBAD24 by a three-point ligation with *ftsA* fragments 1–378 (*Eco*RI-*Xho*I), 399–1260 (*Xho*I-*Pst*I), and pBAD24 (*Eco*RI-*Pst*I).[26] Fragments of *ftsA* were obtained by PCR amplification of the DH5α genomic DNA with the following primers. Fragment 1–378: 5′-CGGAATTCACCATGATCAAGGCGACGGACAG-3′ and 5′-CGCCGCTCGAGATGCTCATCGCGCACACGC-3′. Fragment 399–1260: 5′-CGCCGCTCGAGTATGCGATTGACTATCAGGA-3′ and 5′-AAAACTGCAGTTAAAACTCTTTTCGCAGCCA-3′. Wild-type *ftsA* was cloned using the same terminal oligonucleotides (first and fourth). Fidelity of the cloned inserts was controlled by sequencing both the DNA strands.

Anti-FtsA polyclonal antibodies α_1FtsA were raised in rabbit with purified *E. coli* his-FtsA essentially as described by Harlow and Lane.[28] For western blotting approximately 5×10^6 cells, withdrawn at the indicated times, were loaded onto a 12% SDS-PAGE gel. After resolution, proteins were transferred onto Hybond-ECL filters (Amersham) and treated according to the standard procedure with anti-FtsA antibodies (1:30000). Secondary anti-rabbit HRP-labeled antibodies were added (1:8000), and filters were developed with Enhanced Chemiluminescence (ECL) substrates (Amersham).

Influence of FtsAΔ7 and of FtsA expression on *E. coli* growth rate was studied in DH5α and in XL10GoldKan (Stratagene), both in complete medium (LB: 10 g/L tryptone, 5 g/L yeast extract, 5 g/L NaCl, pH 7.0; Difco) and in M63 minimal medium (13.6 g/L KH_2PO_4, 2 g/L $(NH_4)_2SO_4$,

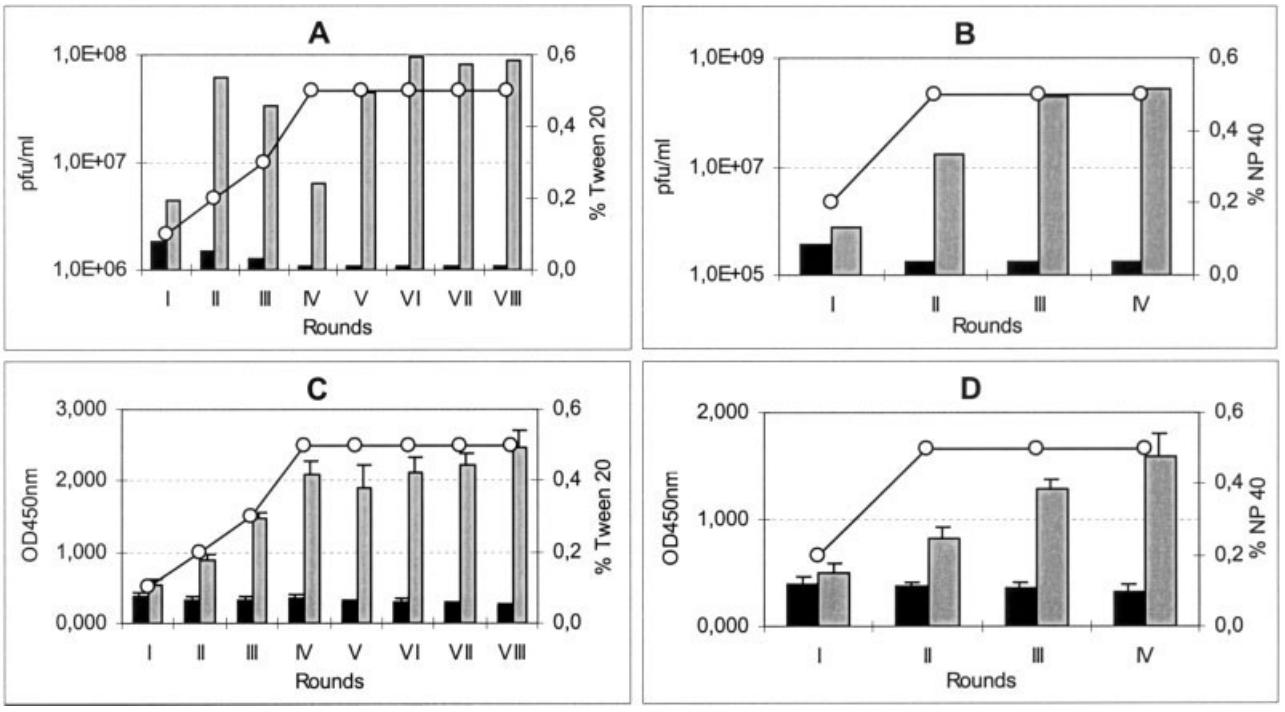

Fig. 1. Affinity selection of Ph.D.-7 bacteriophages with *E. coli* FtsA. (A) Phage panning of his-FtsA was carried out by applying 2×10^{11} pfu per round of Ph.D.-7 library (grey bars) or VCSM13 (black bars) in TBS with a gradual increase of stringency conditions (percentage of Tween 20, line). Phage recovery after each round is reported. (B) Phage panning of his-FtsA was performed as described in (A) in PB with a single-step increase of NP 40 concentration (line). Phage recovery after each round is reported. (C) Affinity of phages recovered after each round of selection in TBS was tested by ELISA with BSA (black bars) and with his-FtsA (grey bars) at the corresponding stringency conditions. Experiment was run in triplicate. (D) Affinity of phages recovered after each round of selection in PB was tested by ELISA with BSA (black bars) and with his-FtsA (grey bars) at the corresponding stringency conditions. Experiment was run in triplicate.

0.5 mg/L $FeSO_4 \times 7H_2O$, 0.2 g/L $MgSO_4 \times 7H_2O$, 0.2% glycerol, 0.5 μg/mL thiamine, 0.1% casaminoacids, pH 7.0, Difco) and almost superimposable results were obtained, thus excluding any possible interference from the genetic background and from the environmental conditions. Precultures were inoculated with cell banks stored at −80°C, grown o.n. at 37°C in the presence of 0.2% glucose, 100 μg/mL ampicillin and subsequently diluted to OD_{600nm} = 0.02 in prewarmed medium with 100 μg/mL ampicillin. Cultures were grown at 37°C until they reached OD_{600nm} = 0.2, then they were split and either induced with 0.2% arabinose or repressed with 0.2% glucose. At the indicated times samples were withdrawn and processed as specified. Microphotographs were taken with a CCD camera (Biorad) connected to an Axioskop HBO 50/AC microscope (Zeiss) at ×1000 magnifications on samples fixed with 0.75% formaldehyde.

Complementation analysis was carried out by growing strains carrying *ftsA(ts)* alleles in NB medium (Oxoid) supplemented with 50 μg/mL thymine (NBT), with 50 μg/mL ampicillin when required and incubated at permissive (30°C) or at restrictive temperature (42°C). Transformants with pBAD24 derivatives were obtained at 30°C, the isolated colonies were inoculated into NBT at 30°C and then plated both onto LB agar with ampicillin (incubated o.n. at 30°C) and on NBT agar (incubated o.n. either at 30°C or at 42°C). A positive complementation result was considered when growth was visible both at 30°C and at 42°C on NBT plates.

RESULTS

Phage Panning of FtsA

The Ph.D.-7 phage-display library, which exhibits random linear heptamers fused to pIII coat protein, was challenged with purified *E. coli* polyhistidine-tagged FtsA under two experimental conditions. First, a gradual stepwise increase of nonionic detergent in a high ionic strength milieu led to the identification of T8A bacteriophages [Tween 20-8 rounds-FtsA; Fig. 1(A)]. Second, a one-step rise of a milder detergent in a lower ionic strength buffer selected the N4A phages [NP 40-4 rounds-FtsA; Fig. 1(B)]. In both cases, enrichment of specific FtsA binders was revealed by the steady increase of phages recovered after every round of panning. This feature was strictly dependent on the presence of the heptamers, since in a control experiment the bacteriophage VCSM13, which lacks any random sequence, was not positively selected [Fig. 1(A,B), black bars]. To unequivocally confirm a specific enrichment of anti-FtsA phages, each round of selection was tested by enzyme-linked immunosorbent assay (ELISA) with FtsA. Results reported on Figure 1(C,D) were consistent with phage recovery data, thus supporting that a selective screening had been achieved. To characterize the

TABLE I. Sequence and Relative Affinity of FtsA-binding Peptides†

Φ	Sequence	Freq.	MurC	FtsA	FtsA/MurC	Φ/VCSM13
T8A-01	FEKYYYW	25	0.313 ± 0.032	3.762 ± 0.144	12.0	18.5
T8A-49	LQPMWFA	1	0.397 ± 0.034	3.491 ± 0.135	8.8	17.2
T8A-28	KVFNWPW	3	0.249 ± 0.016	1.891 ± 0.047	7.6	9.6
T8A-11	KLWVIPQ	2	0.315 ± 0.021	2.081 ± 0.027	6.6	10.5
N4A-07	LTYRISP	1	0.277 ± 0.027	1.828 ± 0.066	6.6	9.2
N4A-01	LSLPKLP	2	0.345 ± 0.037	2.003 ± 0.047	5.8	10.1
T8A-19	FQNNLQL	1	0.230 ± 0.009	1.335 ± 0.039	5.8	6.9
N4A-30	GSFYVFP	1	0.228 ± 0.009	1.185 ± 0.046	5.2	6.2
N4A-04	LVYPPMV	1	0.290 ± 0.026	1.423 ± 0.025	4.9	7.4
N4A-21	ITPYTVL	1	0.342 ± 0.015	1.301 ± 0.049	3.8	6.8
N4A-10	LPPLNYY	1	0.276 ± 0.009	0.801 ± 0.073	2.9	5.8
N4A-05	HYTSATL	1	0.212 ± 0.017	0.552 ± 0.022	2.6	5.7
N4A-24	WQPNTRP	1	0.280 ± 0.013	0.728 ± 0.031	2.6	5.2
N4A-26	YNPLPGT	3	0.275 ± 0.013	0.716 ± 0.064	2.6	5.4
T8A-06	TDRPALS	8	0.301 ± 0.031	0.752 ± 0.054	2.5	5.1
N4A-19	APLESNW	2	0.280 ± 0.022	0.672 ± 0.044	2.4	4.3
N4A-08	IPRTYPL	1	0.272 ± 0.008	0.625 ± 0.010	2.3	3.2
N4A-22	SAPGLLH	1	0.267 ± 0.014	0.615 ± 0.038	2.3	4.4
N4A-12	DYHNHLT	1	0.279 ± 0.020	0.586 ± 0.051	2.1	3.8
N4A-16	SPTQSTL	1	0.276 ± 0.019	0.580 ± 0.041	2.1	4.1
N4A-29	AQAIMQY	1	0.246 ± 0.013	0.517 ± 0.051	2.1	4.5
T8A-30	HHVKFQN	1	0.297 ± 0.014	0.623 ± 0.064	2.1	4.1
N4A-14	SLCSVLC	1	0.290 ± 0.030	0.580 ± 0.012	2.0	4.3
N4A-13	HTTYFPM	1	0.190 ± 0.008	0.552 ± 0.024	2.9	5.6
N4A-27	HVLPPLH	1	0.289 ± 0.009	0.810 ± 0.056	2.8	5.6
N4A-11	LHAWQDL	1	0.286 ± 0.016	0.773 ± 0.045	2.7	5.2
N4A-02	TGNPPPN	1	0.287 ± 0.026	0.745 ± 0.070	2.6	5.5
N4A-17	LSNYTRP	1	0.274 ± 0.018	0.712 ± 0.038	2.6	5.0
N4A-09	HTPLATA	1	0.287 ± 0.011	0.718 ± 0.037	2.5	4.9
N4A-15	HMPNASF	1	0.279 ± 0.017	0.697 ± 0.043	2.5	4.8
N4A-25	YNPYTPL	1	0.268 ± 0.024	0.670 ± 0.046	2.5	4.8
T8A-02	VMQATHD	5	0.255 ± 0.013	0.612 ± 0.078	2.4	5.3
T8A-08	WHTNYEP	3	0.251 ± 0.014	0.603 ± 0.065	2.4	4.8
N4A-03	STLLPES	1	0.300 ± 0.023	0.690 ± 0.061	2.3	3.9
N4A-20	NVNLLLP	1	0.276 ± 0.023	0.635 ± 0.022	2.3	4.5
N4A-06	QANPLMI	1	0.289 ± 0.012	0.636 ± 0.019	2.2	4.2
N4A-23	NTTTYPT	1	0.277 ± 0.023	0.525 ± 0.038	1.9	4.4

†Φ, bacteriophage displaying the selected peptide; sequence, amino acid sequence of the heptapeptides; Freq., frequency of recurrence of each peptide among the sequenced bacteriophages; MurC, average ELISA values (OD_{450nm}) ± standard deviation (n = 4) of each phage with MurC as target; FtsA, average ELISA values (OD_{450nm}) ± standard deviation (n = 4) of each phage with his-FtsA as target; FtsA/MurC, ratio between the ELISA values of each phage challenged with his-FtsA and his-MurC, respectively; Φ/VCSM13, ratio between the ELISA values to his-FtsA of each recombinant phage (Φ) with respect to the negative control VCSM13. High-affinity binding phages are separated from low-affinity binding phages.

selected clones, 90 individual plaques were randomly picked and the amino acids of the variable heptapeptides were deduced from their corresponding nucleotide sequences (Table I). The analysis revealed that the selected phages represented 37 unique clones. To judge their individual binding properties, we tested by ELISA their selectivity, i.e., their ability to discriminate between FtsA and the unrelated proteins BSA and his-MurC (Fig. 2 and Table I, "FtsA/MurC"), and their relative affinity, *i.e.* the strength of their binding to FtsA with respect to the negative control, the wild-type bacteriophage VCSM13 (Fig. 2 and Table I, "Φ/VCSM13"). As a result, 10 phages were found to bind FtsA with high affinity and specificity and they were further characterized. Any possible recognition of the polyhistidine tail was ruled out, since they displayed a negligible affinity to histidine-tagged MurC, an unrelated protein harboring the same N-terminal tag (Fig. 2; white bars). It should be noted that only for few phages the relative affinity correlated with their frequency of recovery (e.g., T8A-01. See Fig. 2 and Table I). This was somehow expected: in fact, although ELISA results can provide an estimate of the inherent binding property of each phage, the frequency of recovery is affected by several additional factors, including replication advantage, translation and folding bias, pIII coat stability and retained infection efficiency.

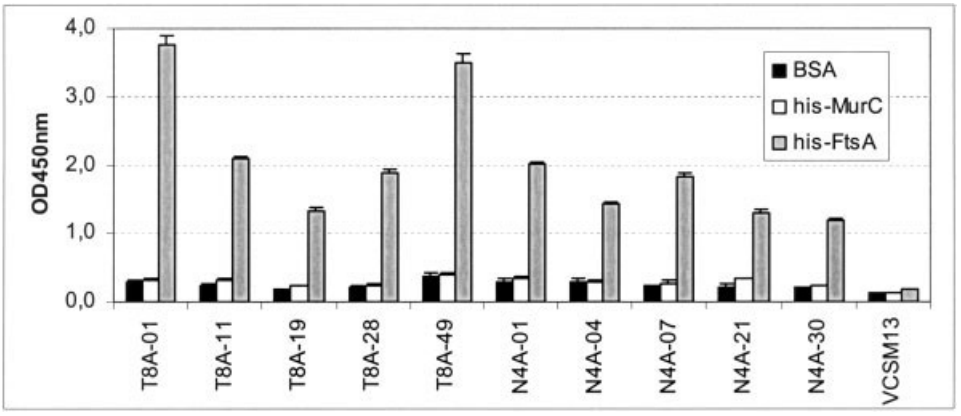

Fig. 2. ELISA of high-affinity bacteriophages. Each high-affinity bacteriophage was challenged with BSA (black bars), with his-MurC (white bars), and with his-FtsA (grey bars), respectively. VCSM13 was also included as negative control. The experiment was performed in quadruplicate.

Analysis of the Peptide Sequences

Comparison of the overall amino acid composition of the high-affinity heptapeptides with the corresponding frequencies of the original library revealed that some residues were particularly enriched (W,Y,K,F,V), whereas other were significantly depleted (A,R,S,G) or completely omitted (H,D,C) [Fig. 3(A)]. Conversion of the sequences with dedicated SIMPLIFY program based on physicochemical properties of the amino acids allowed the definition of a degenerate consensus sequence. Briefly, residues were grouped in hydrophobic (Ø: F,Y,W,L,V,I,M), neutral (‡: A,T,G,S), hydrophilic (#: Q,N,K,R,E), prolin residues (P) and then aligned with CLUSTALW.[29,30] Figure 3(B,C) shows that the tripartite consensus sequence is formed by a N-terminal hydrophilic region followed by a hydrophobic core closed at the C-terminus by a prolin residue. Sequences displayed by the low-affinity bacteriophages comply more weakly with the consensus in respect with the high-affinity binders (Table I). The fact that the selected peptides conform to a consensus sequence suggests that they all recognize a unique binding site on FtsA.

Because peptide displayed by phage libraries has been widely used to infer protein ligands of target molecules,[22,23] we searched the databases for similarity with the high-affinity peptide sequences.[31] Conventional BLASTP search on *E. coli* database did not retrieve either known interacting partners of FtsA, nor other proteins involved in cell division. Only when T8A-11 sequence (KLWVIPQ) was submitted, FtsA itself appeared among the best hits.[31] The degree of homology with the parental sequence is remarkable: 62.5% of identity and 78.5% of similarity with residues 126–133 (RVLHVIPQ). This region of FtsA is located on subdomain 1C and is exposed on the surface of the molecule.[19] This evidence strongly suggested that residues 126–133 are involved in FtsA homodimerization, because sequence of T8A-11 was affinity selected to interact with FtsA.

Correlated Mutation Analysis

The identification by phage panning of amino acids 126–133 as putative determinants of FtsA homodimerization did not give information on which residues are contacted by these amino acids and how the two molecules of FtsA are arranged in the homodimer. To shed light on these issues, a correlated mutation analysis of FtsA orthologues was performed. Correlated mutations arise in protein sequences to compensate substitutions that independently occur during evolution. As residues in physical contact are subjected to a high selective pressure to compensate for substitutions, this analysis predicts protein contacts, both for inter-domain docking and for intermolecular interactions.[34,37]

Multiple sequence alignment of orthologous FtsA proteins was analyzed using PLOTCORR program and the obtained amino acid pairs were compared with their respective position in the crystal structure of FtsA from *T. maritima*.[19,32] A particularly notable correlation (average correlation coefficient $r_i = 0.62$) was found between a group of residues encompassing the ATP-binding site and amino acids 138–151 of the loop connecting S6–S7 strands in subdomain 1C (Table II). Remarkably, the region of homology with peptide T8A-11 flanks at the immediate N-terminus this loop [Fig. 4(A,B)]. Therefore, correlated mutation analysis converged to identify subdomain 1C as an interacting interface of FtsA dimerization. Multiple sequence alignment of the orthologous FtsA proteins of this region displays a good compliance with the peptide consensus motif, which appears as one of the best conserved in evolution outside the ATP-binding site, thus supporting its functional relevance (Fig. 5). Taken together, all these evidences indicate that residues 126-133 (homologous to T8A-11 peptide) and 138–151 (correlated mutation pairs) of subdomain 1C have a role in FtsA self-interaction.

A Model for the Homodimerization of FtsA

On the basis of this information, we propose a model for the homodimerization of FtsA. In the model plotted in Figure 4(C), the first FtsA molecule (blue) inserts its subdomain 1C into the groove of the second monomer (red) formed by the intersection of the upper flat surface of subdomain 1A, the loops surrounding helix H9 of subdo-

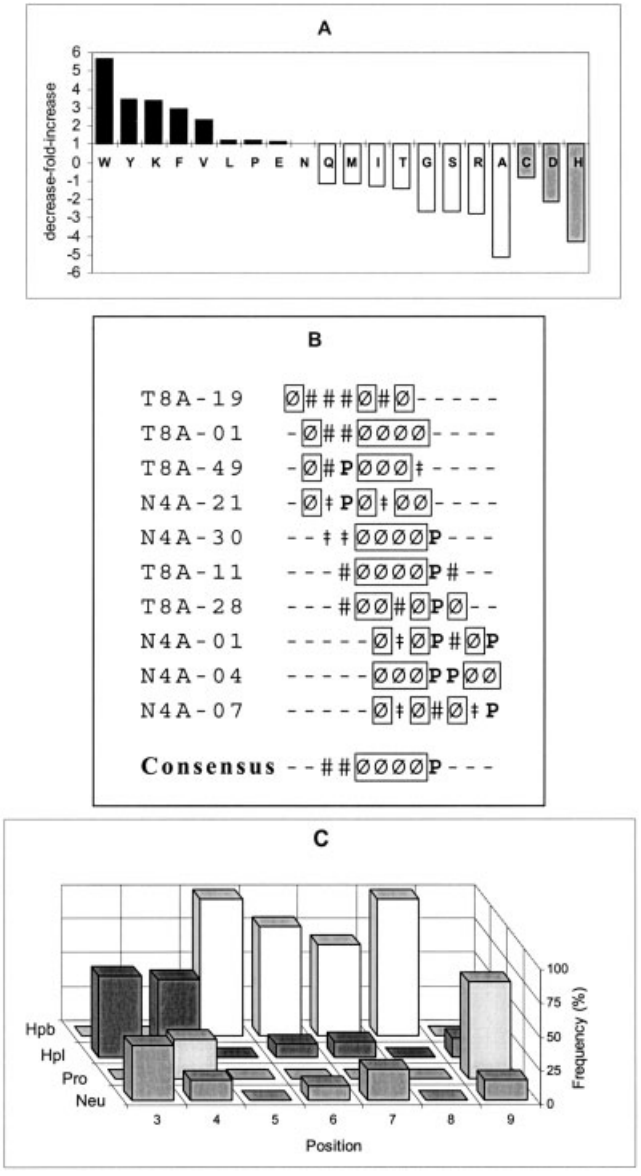

Fig. 3. Sequence analysis of the high-affinity binding peptides. (A) Relative amino acid abundance in the high-affinity heptapeptides directed against FtsA. Composition of the 10 heptapeptides was compared with amino acid frequency of Ph.D.-7 library. The fold increase (black bars) and fold decrease (white bars) are shown. Cysteine, aspartic acid and histidine (C,D,H) residues are completely absent in the selected peptides (grey bars). (B) FtsA-binding peptides were aligned after sequence transformation with SIMPLIFY program. Ø: F,Y,W,L,V,I,M (hydrophobic, boxed); ‡: A,T,G,S (neutral); #: Q,N,K,R,E (hydrophilic); P: prolin. The degenerate consensus is indicated (bottom). (C) Distribution of amino acid residues at each position of the alignment shown in (B). Hydrophobic residues (Hpb: F,Y,W,L,V,I,M; white bars) are enriched at positions 5-8, hydrophilic residues (Hpl: N,Q,K,R,E; black bars) at positions 3-4, whereas prolin (Pro: light grey bars) at position 9. Neutral residues (Neu: A,T,G,S) are indicated as dark grey bars.

TABLE II. Correlated Mutation Analysis

Subdomain 1C	Active site	Correlation Coefficient r_i
D138	S43	0.548
	R300	0.892
	G336*	0.892
Q140	H87	0.616
	S192*	0.515
	E303	0.531
G142	I15	0.504
	G213	0.515
K144	G236	0.507
P146	G37	0.641
	G39	0.578
	S43	0.618
	G45	0.795
	M46	0.674
	D242	0.796
	R300	0.687
	G336*	0.687
V147	G236	0.618
L149	S43	0.513
	G45	0.567
	D47	0.508
	D242	0.745
	R300	0.734
	L334	0.581
	G336*	0.734
G151	I35	0.529
	G37	0.690
	S43	0.550
	G45	0.563
	M46	0.502
	A64	0.515
	E69	0.508

†Correlation coefficients r_i corresponding to pairs of residues present in subdomain IC related to those surrounding the ATP-binding site. Values were obtained by using the program PLOTCORR. Asterisks indicate that amino acids S192 and G336 are targeted in lethal conditional mutants *ftsA40* and *ftsA102,* respectively.

main 2A, and by the barbed end of subdomain 2B. This arrangement orients residues 126–133 (yellow) of the upper monomer in close proximity to the apical strands S12–S13 of the second monomer, while amino acids 138–151 (red spheres), lying in the loop connecting S6–S7, face the correlated pairs in subdomain 1A of the lower FtsA molecule (green spheres) close to the ATP-binding site.

To probe the accuracy of the proposed model, 5×10^3 alternative docking solutions were generated with the program GRAMM and analyzed with two different approaches.[33] First, the distance between the correlated residues was corrected by the correlation coefficient obtained by the program PLOTCORR to give more weight to pairs of amino acids with a higher correlation coefficient.[32] Finally, a "correlated mutations-corrected distance" factor (*cd*) for each individual solution was calculated (see Materials and Methods).[34] Figure 6(A) shows the distribution of the *cd* values, where the low *cd* value of the proposed model (black arrow) indicates a good correlation with contacts predicted by calculation of correlation coefficients.

A second evaluation of accuracy was performed by using the harmonic average factor (*Xd*).[34] This factor estimates not only physical contacts between residues, but also performs a continuous measurement of proximity taking into account

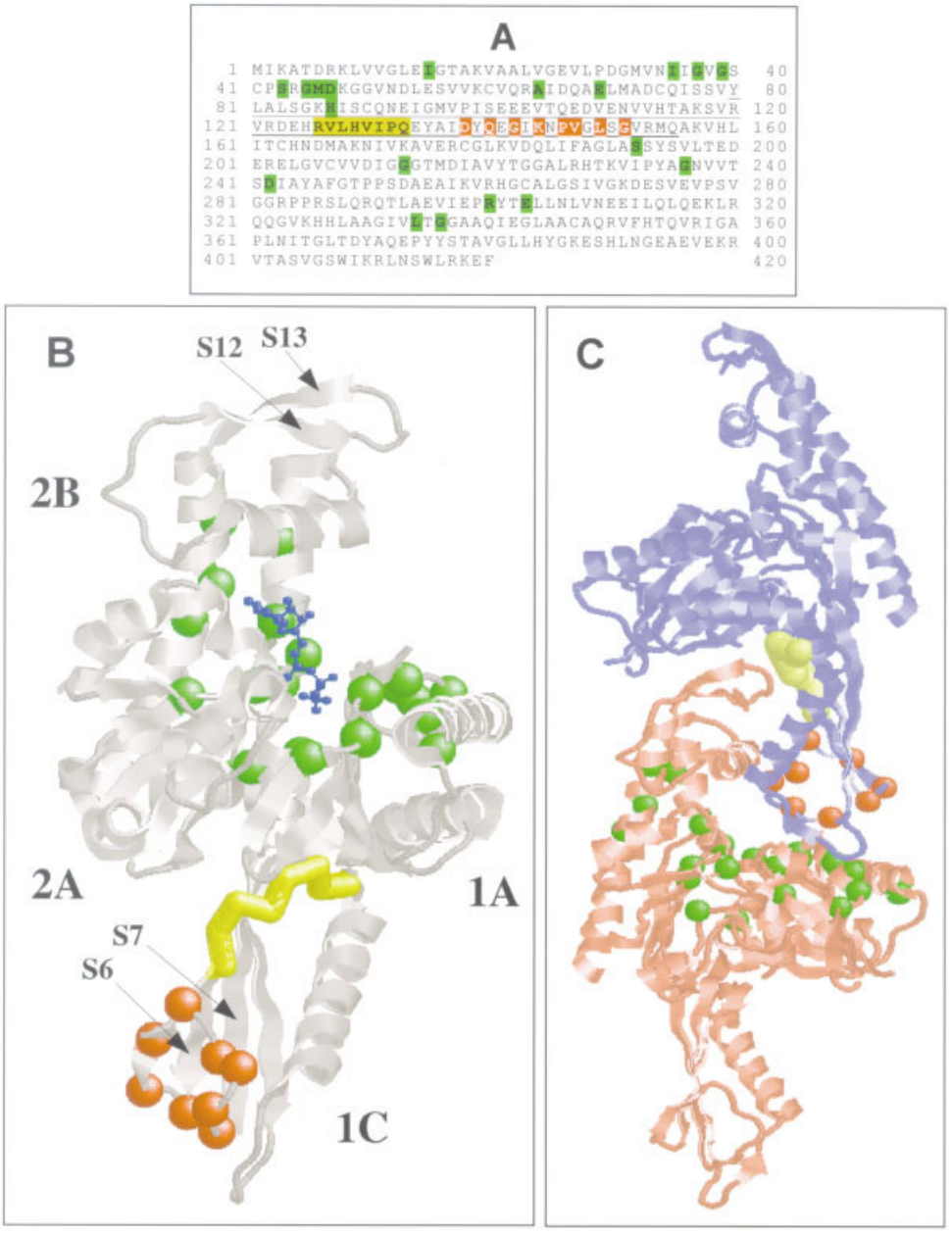

Fig. 4. A model for FtsA homodimerization. (A) Amino acid sequence of *E. coli* FtsA. Residues of subdomain 1C are underlined. Region homologous to T8A-11 peptide is bolded with a yellow background. Correlated pairs of amino acids belonging to subdomain 1C are depicted with a red background, whereas their counterparts have a green background. (B) Ribbon plot of FtsA crystal structure. The structure is divided into four subdomains 1A, 1C, 2A, 2B. Positions of strands S6–S7 and S12–S13 are indicated. The correlated amino acid pairs in the loop connecting the S6–S7 strands are depicted as red spheres, whereas their counterparts surrounding the active site are depicted as green spheres. The ATP molecule is drawn in blue. The region homologous to peptide T8A-11 is represented as yellow backbone. (C) Ribbon plot of the proposed model of a FtsA homodimer. The first molecule of FtsA (blue, top) inserts its subdomain 1C into the cleft made by subdomains 2B, 2A, and 1A of the second molecule (red, bottom). The region of the first monomer homologous to T8A-11 peptide (yellow backbone) contacts the loop connecting strands S12–S13 of the second monomer, while the correlated mutation residues on loop between strands S6–S7 (red spheres) are located in close proximity with their counterparts on the facing monomer (green spheres).

the distance of both the correlated pairs and all pairs of positions. Briefly, the distances between pairs of residues were grouped in bins of 4 Å for each of the previous 5×10^3 docking solutions, obtaining two different distributions of binned data for the indicated correlated pairs and for all pairs of positions. The difference between the two distribu-

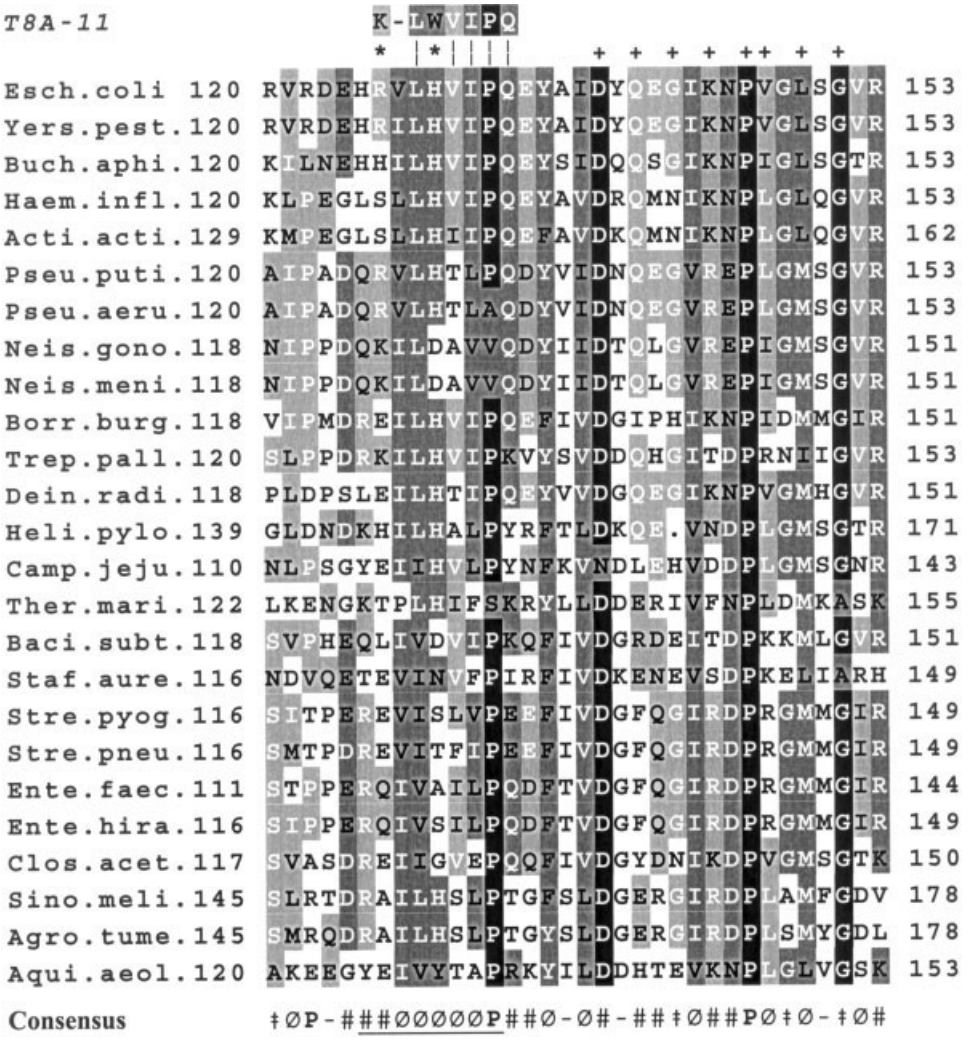

Fig. 5. Sequence alignment of subdomain 1C of orthologous FtsA proteins. Sequences were aligned by using the following notation. Backgrounds: black, invariant position (>85%); dark grey, highly conserved (>65%); light grey, moderately conserved (>40%); white, nonconserved. Fonts: black, conservative substitution; white, consensus. Peptide T8A-11 is displayed on top showing identities (¦) and conservative substitutions (*). Symbols (+) on top indicate the position of the correlated mutation residues. Consensus sequence in the T8A-11 homologous region is indicated on bottom following the notation of Fig. 3 and consensus sequence corresponding to residues 126–133 is underlined. Esch.coli: *Escherichia coli*. Yers.pest.: *Yersinia pestis*. Buch.aphi.: *Buchnera aphidicola*. Haem.infl.: *Haemophylus influenzae*. Acti.acti.: *Actinobacillus actinomycetemcomitans*. Pseu.puti.: *Pseudomonas putida*. Pseu.aeru.: *Pseudomonas aeruginosa*. Neis.gono.: *Neisseria gonorrhoeae*. Neis.meni.: *Neisseria meningitidis*. Borr.burg.: *Borrelia burgdorferi*. Trep.pall.: *Treponema pallidum*. Dein.radi.: *Deinococcus radiodurans*. Heli.pylo.: *Helicobacter pylori*. Camp.jeju.: *Campylobacter jejuni*. Ther.mari.: *Thermotoga maritima*. Baci.subt.: *Bacillus subtilis*. Staf.aure.: *Staphylococcus aureus*. Stre.pyog.: *Streptococcus pyogenes*. Stre.pneu.: *Streptococcus pneumoniae*. Ente.faec.: *Enterococcus faecalis*. Ente.hira.: *Enterococcus hirae*. Clos.acet.: *Clostridium acetobutilicum*. Sino.meli.: *Sinorhizobium meliloti*. Agro.tume.: *Agrobacterium tumefaciens*. Aqui.aeol.: *Aquifex aeolicus*.

tions was calculated bin by bin and normalized to increase weight of closer distances (see Materials and Methods). The higher the *Xd* value, the lower is the distribution of distances of the correlated pairs. Therefore, the actual protein-protein arrangement tends to show a *Xd* value higher than the majority of the docking solutions.[34] Figure 6(B) shows that the *Xd* value for the proposed model (black arrow) is located among the highest scores of all the 5×10^3 alternative docking solutions, confirming once more a good accuracy of the dimerization model.

Protein–Protein Interaction Residues

Prediction of amino acids involved in protein-protein interactions allows characterizing protein domains and discriminating among docking models. To probe the accuracy of our model, we performed an analysis to detect protein–protein interaction residues in the framework of a neural network. This system combined the evolutionary information accumulated in sequence profiles derived from family alignments with structural data of the surface

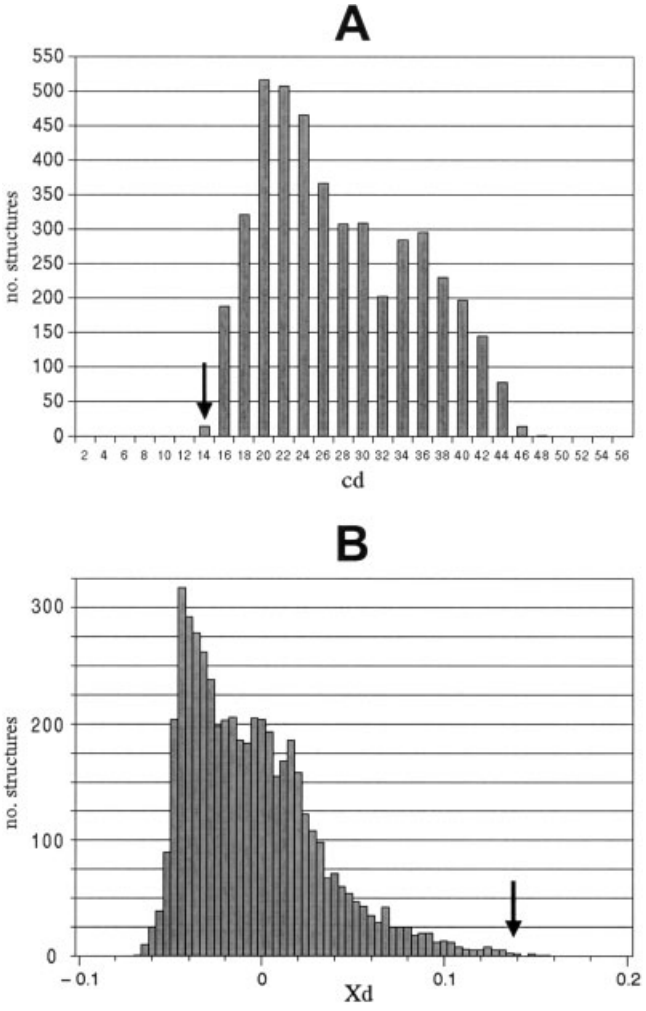

Fig. 6. Validation of the homodimerization model. (A) Distribution of the "correlated mutations-corrected distance" values (*cd*) obtained for 5×10^3 alternative docking solutions. The *y*-axis represents the number of docking solutions corresponding to each *cd* value. The *x*-axis represents the *cd* values grouped in bins of two units. The arrow indicates the position of the *cd* value for the proposed model. (B) Distribution of the harmonic average factor values (*Xd*) obtained for the same structural solutions as in (A). The black arrow indicates the position of the *Xd* value calculated for the proposed model.

patches identified as sets of neighbor residues exposed to solvent.[35,36] In brief, the neural network was trained with a large set of dimer-forming pairs of known interacting proteins extracted from the SPIN database, and it used as input both 3D coordinates from Protein Data Bank entries and multiple sequence alignments from the HSSP database (see Materials and Methods). The output consisted of a list of surface residues predicted as interacting determinants of the protein (positive contacts; Table III). Once these residues were mapped on the homodimerization model, some interesting features were immediately evident. First, approximately two thirds of the contact residues are distributed on two regions matching exactly the model proposed for the homodimerization of FtsA (Fig. 7; gold spheres). These regions are located on the interface

TABLE III. Residues of FtsA Predicted to be Involved in Protein-Protein Interaction†

Region I		Region II		Not I or II	
V10 (4)	V79 (1)	I36 (2)	M71 (1)	N34 (5)	C90 (1)
L81 (3)	**V130*** (3)	I358 (2)	L362 (3)	Q91 (2)	N92 (3)
I131* (2)	L383 (6)	D369 (2)	A371 (2)	K230 (4)	V231 (1)
Y385 (7)		Q372 (7)	Y375 (2)	P233 (1)	A329 (3)

†Amino acids obtained from the protein interaction analysis were arranged in three regions according to their spatial distribution in the proposed model for FtsA dimerization. Region I comprises residues facing subdomain 2B of the accompanying FtsA molecule, while Region II groups amino acids proximal to subdomain IC of the attendant monomer. Asterisks on bolded V130 and I131 indicate their position within the T8A11-homologous region. Numbers in parentheses indicate neural network reliability index for positive contacts.

between subdomains 2B-1A (Region I) and 1A-1C (Region II) of the facing monomers [Fig. 7(B)]. More strikingly, two residues among the amino acids predicted to be involved in protein-protein interactions are precisely V130 and I131, which belong to the T8A11-like sequence RVLHVIPQ (Fig. 7, magenta spheres). In conclusion, an independent approach converged to support the reliability of the predicted model for the homodimerization of FtsA.

ftsAΔ7, a Deletion Mutant Lacking Amino Acids 126–133

Functional role of residues 126–133 of FtsA was examined by producing an in frame site-directed deletion mutant lacking this region of the protein (Fig. 8). We placed the internally deleted gene *ftsAΔ7* under the control of a P_{BAD} promoter in a pBAD24 vector (pBAD-FtsAΔ7). This expression system is elective for both overexpression studies and complementation analysis, because transcription from P_{BAD} promoter can be finely tuned over a wide range of inducer concentrations or completely silenced by the repressor.[26]

To assess whether the deletion caused an alteration in protein structure such that it became completely unfolded or degraded, we analyzed the effects of overexpression of FtsAΔ7 in comparison with wild-type FtsA (pBAD-FtsA). In time-course experiments, FtsA and FtsAΔ7 showed a comparable expression profile when analyzed by Western blotting (Fig. 9). The expression was confirmed to be tightly controlled, because basal level and repressed state were under the detection threshold (lanes 1 and 8). This experiment shows that protein degradation was not significant, allowing further characterization of the cellular effects produced by the recombinant proteins. The overexpression of FtsA and FtsAΔ7 had a dramatic impact on cell growth. Induction of the two proteins promptly caused a significant drop of the growth rate, which ultimately ended in a complete arrest [Fig. 10(A)]. This behavior was expected for overexpression of wild-type FtsA, because its cellular ratio can not be altered without blocking cell division.[7] To determine whether this phenotype was mediated by a bacteriostatic or a bactericidal mechanism, we quantitatively estimated the killing effect of the expression of the two FtsA proteins by plating serial dilutions of

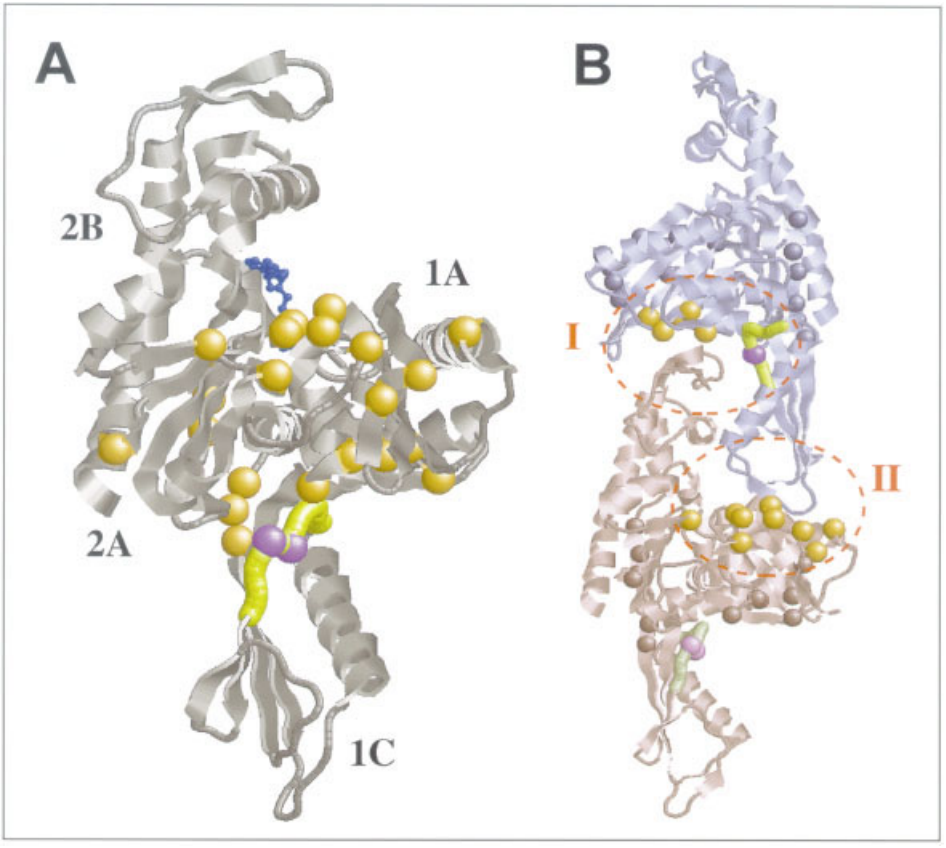

Fig. 7. Mapping of FtsA residues predicted to be involved in protein-protein interaction. (A) Ribbon plot of the crystal structure of FtsA. Residues involved in protein-protein interaction are depicted as gold spheres. Amino acids V130 and I131, also predicted as interacting residues, are drawn as magenta spheres indicating their position within the T8A11-homologous region (yellow backbone). The ATP molecule is depicted in blue. (B) Proposed model for the homodimerization of FtsA. The predicted interacting residues of both monomers are colored in gold and grouped in two regions, marked as I and II, respectively. The position of amino acids V130 and I131 and of the T8A11-homologous region are indicated as in (A).

FtsA

364 -cgcgatgagcat **cgtgtg**ctg**catgtgatcccgcaa** gagtatgcgatt- 411

122 -RDEH **RVLHVIPQ** EYAI- 137

FtsAΔ7

122 -RDEH L EYAI- 130′

364 -cgcgatgagcat ctc gagtatgcgatt- 389′

Fig. 8. Sequences of wild-type FtsA and of FtsAΔ7. Top: DNA and amino acid sequence of wild-type FtsA from *E. coli* in the region homologous to T8A-11. Amino acids and nucleotides which are deleted in the mutant FtsAΔ7 protein are bolded. Bottom: The heptapeptide homologous to T8A-11 is deleted in FtsAΔ7. Hyphens indicate the new notation of nucleotides and amino acids in FtsAΔ7. The newly inserted *Xho*I site is underlined.

the induced and of the repressed cultures. Figure 10(B) shows that viability of cells expressing FtsA and FtsAΔ7 decreased steadily with induction time, reaching a difference in respect with their repressed negative controls up to 10^6 colony-forming units. Effects of the overexpression of FtsAΔ7 matched those of FtsA also as far as cell phenotype is concerned. Under microscopic examination, induction of FtsAΔ7 gave rise to long nonseptate filamentous cells [Fig. 10(C,b)], which were almost indistinguishable from cells expressing the wild-type protein [Fig. 10(C,c)]. As negative controls, cells transformed with pBAD24 and with the same vector bearing the gene encoding for MBP were analyzed in parallel, confirming that lethality and filamentation were exclusively associated with the expression of FtsA and FtsAΔ7 (data not shown).

The experiments shown in Figure 10 demonstrated that expression at high level of FtsAΔ7 led to cellular effects similar to those obtained with the wild-type protein. These results can be explained only by assuming that FtsAΔ7 is properly folded *in vivo*, because deletion of amino acids 126–133 preserved, if not even slightly increased, the cellular toxicity of FtsA overexpression.

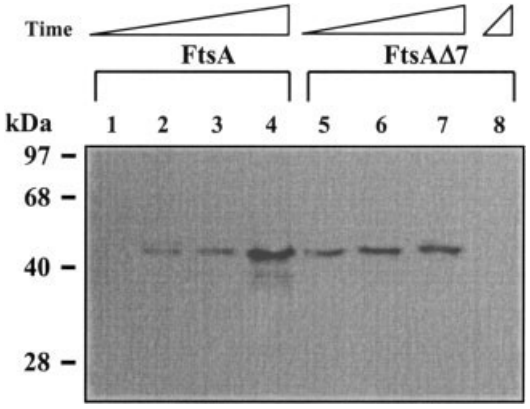

Fig. 9. Expression of FtsA and FtsAΔ7 during cell growth. Total protein extracts (1 μg/lane) of *E. coli* XL10GoldKan harboring pBAD-FtsA (1–4) or pBAD-FtsAΔ7 (5–8) were analyzed by Western blotting with anti-FtsA antibodies. Samples were withdrawn immediately before induction (lane 1) and 2-h (lanes 2 and 5), 4-h (lanes 3,6), and 6-h postinduction with 0.2% arabinose (lanes 4 and 7) or repression with 0.2% glucose (lane 8).

Amino Acids 126–133 Are Essential

To assess the functional relevance of amino acids 126–133 we evaluated the ability of *ftsAΔ7* to complement either a thermosensitive missense *ftsA* allele (*ftsA2*; D2 strain) or an amber mutation of *ftsA* in a temperature-sensitive suppressor background (*ftsA16*; OV16 strain).[24,25] These two strains were transformed with pBAD24 carrying wild-type *ftsA* or *ftsAΔ7*. Their ability to grow at permissive (30°C) and at nonpermissive temperature (42°C) was tested by inducing expression of FtsA and FtsAΔ7 at physiological level (0.02% arabinose) and at overexpressed level (0.2% arabinose). The result of complementation assay is summarized in Table IV. As expected, wild-type FtsA was able to rescue the conditional-lethal phenotype of D2 and OV16 strains at the non-permissive temperature only when expressed at low levels, because its overexpression caused filamentation and lethality.[7] On the contrary, FtsAΔ7 failed to recover the lethal phenotype of both strains when grown under restrictive conditions at any expression level, thus demonstrating that amino acids 126–133 are essential for FtsA activity and hence for *E. coli* cell division.

DISCUSSION

In this work we propose a model for the self-interaction of *E. coli* FtsA, based on the similarity of peptides selected by phage panning with a subdomain region of FtsA itself and on the analysis of the correlated mutations occurring in the orthologous sequences of FtsA. The accuracy of this model was validated with different approaches. First, a large number of alternative docking solutions was probed, confirming that the proposed model is in substantial agreement with the position of the putative contact points of the two facing molecules. In addition, mapping of residues predicted as determinants of inter-molecular contacts provided support for the proposed relative orientation of the two FtsA molecules in the homodimer. Finally, the functional relevance of region 126–133 of subdomain 1C was unequivocally demonstrated by the lethal phenotype of the *ftsAΔ7* mutant.

It is worthy to be mentioned that our analysis did not retrieve the 27 C-terminal residues of FtsA, which had been demonstrated by genetic and functional approaches to have an essential role in FtsA homodimerization.[16] This discrepancy is probably due to the flexible nature of the terminal part of FtsA, which also made impossible its solution in the crystal structure.[19] Nevertheless, position of the C-terminal tail is most likely oriented on the same direction and in close proximity to subdomain 1C.[19] Therefore, this subdomain and the extreme C-terminal part of FtsA could both contribute to the formation of the interacting interface.

Despite the different orientation of subdomain 1C, the mutual disposition of the FtsA molecules in the proposed model shares many similarities with the arrangement of the actin monomers in the polymerized form. In fact, subdomain 1C of one monomer of FtsA occupies in the homodimer the space corresponding to the structurally related subdomain 1B of actin.[38] Moreover, sets of amino acids that are proposed in our model to directly contact the facing FtsA molecules have corresponding functional counterparts in actin. For instance, the loop connecting S11–S12 strands of subdomain 2B in actin, which is structurally equivalent to the loop linking S12–S13 strands in FtsA (contacted by the T8A11-homologous motif), was demonstrated to be involved in actin polymerization by site-directed mutagenesis, e.g., actin mutant G245D/K has a negligible polymerization activity, and by analysis of crystal structures of the actin molecule.[38–40] On the other hand, the loop connecting strands S4–S5 in actin subdomain 1B, corresponding to the loop between strands S6–S7 in subdomain 1C of FtsA (the correlated mutation pairs), was directly implicated in actin self-interaction by covalent derivatization studies—polymerization is severely affected by targeting H40, Q41 and K50—by characterization of temperature-sensitive mutants (R37A, R39A, K50A, D51A) and by stereoplot analysis of the actin three-dimensional structure.[38–40] As in actin, the proposed model is consistent with the assembly of FtsA units in polymers. In particular, the disposition of the FtsA molecules in the polymerized form is reminiscent of the ribbon structure in actin, where extensive contacts organize adjacent monomers with an alternate symmetry along a screw axis.[40]

Amino acid counterparts of the correlated mutations on subdomain 1C encompass the ATP-binding site on the facing monomer. Genetic analysis provided a wide set of lethal-conditional alleles of *ftsA*, which contributed to define functional domains of the protein. It is noteworthy that among them *ftsA40* and *ftsA102* display point mutations that target residues belonging to the correlated pairs. In particular, *ftsA40* (S192L) encodes a temperature-sensitive protein, whereas *ftsA102* (G336D) encodes a nonfunctional protein (see Table II).[6] Although these two amino acids are located close to the active site, they are not directly involved in nucleotide binding.[19] Rather, muta-

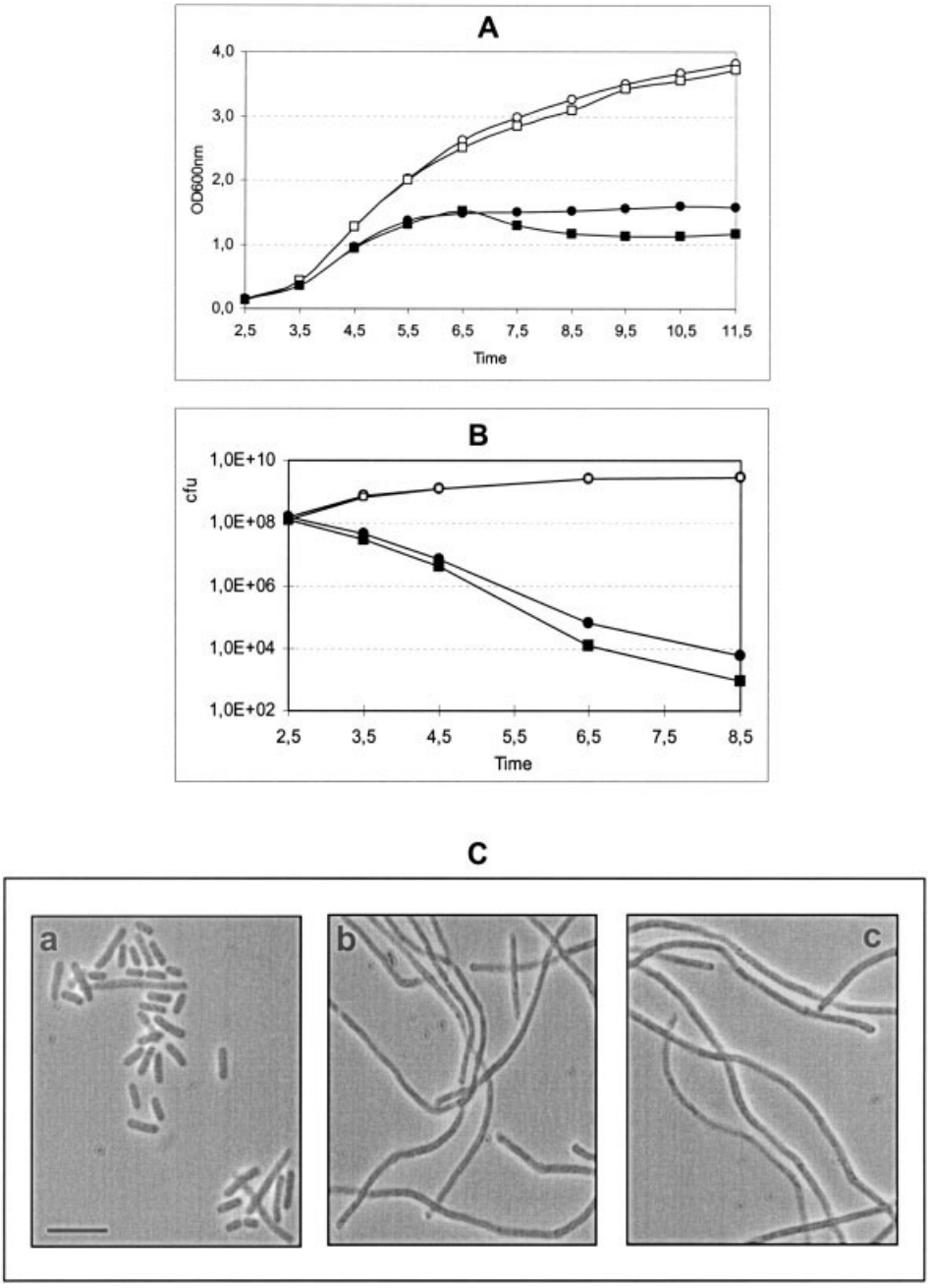

Fig. 10. Effects of FtsA and FtsAΔ7 overexpression on *E. coli* growth rate and viability. (A) Early exponential phase *E. coli* XL10GoldKan cells harboring pBAD-FtsA (circle) or pBAD-FtsAΔ7 (square) were split into duplicate cultures, one induced with 0.2% arabinose (solid) and the other repressed with 0.2% glucose (open). The growth rates (OD_{600nm}) were determined over a 9-h period post-induction. (B) Samples of *E. coli* XL10GoldKan harboring pBAD-FtsA (circle) and pBAD-FtsAΔ7 (square) were withdrawn before induction (2.5 h) and 1, 2, 4 and 6 h after induction with 0.2% arabinose (solid) or repression with 0.2% glucose (open), serially diluted and plated on LB containing 100 μg/mL ampicillin, 1% glucose. Viability was measured by counting the colony forming units (cfu). (C) Microphotographs of *E. coli* XL10GoldKan harboring pBAD-FtsAΔ7 were taken before induction (a) and 6 h postinduction with 0.2% arabinose (b). Expression of FtsAΔ7 gave rise to long nonseptate cells, which were almost indistinguishable from cells harboring pBAD-FtsA after the same period of induction (c). Bar in microphotograph (a): 10 μm.

tions occurring at these positions are expected to alter the geometry of the active site, indirectly reducing the affinity for ATP, as it was demonstrated for *ftsA102*.[6] Conversely, coordinated changes of these positions in the orthologous proteins with amino acids which reside in the facing subdomain 1C suggest that a mutual interplay can exist between homodimerization and nucleotide binding. Moreover, crystal structure of FtsA from *T. maritima* revealed

TABLE IV. Complementation Analysis of *ftsA* and *ftsAΔ7*[†]

ftsA				*ftsAΔ7*			
		E. coli strains				*E. coli* strains	
Temp.	Inducer	D2	OV16	Temp.	Inducer	D2	OV16
30°C	0	+	+	30°C	0	+	+
	0.02%	+	+		0.02%	+	+
	0.2%	−	−		0.2%	−	−
42°C	0	−	−	42°C	0	−	−
	0.02%	+	+		0.02%	−	−
	0.2%	−	−		0.2%	−	−

[†]Complementation of *E. coli* strains OV16 and D2 either with wild-type *ftsA* or with *ftsAΔ7*. When FtsA is expressed at low level (0.02% arabinose) at nonpermissive temperature (42°C), it is able to revert the lethal conditional phenotype of both strains (+). On the contrary, expression at any level of FtsAΔ7 does not complement their temperature-sensitive phenotype (−).

that the connection of subdomain 1C with the rest of the protein is flexible, with an angle of rotation of 13.5°.[19] Although flexibility could not be exclusively related to ATP-binding, van den Ent and Löwe proposed that binding of the nucleotide may fix subdomain 1C in a specific position, modifying the width of the cleft between subdomains 1A and 1C.[19] Here we present molecular and combinatorial evidences which postulate that subdomain 1C interacts with a group of amino acids surrounding the active site of the opposite monomer. Mutations targeting two of these amino acids (S192L and G336D) are expected to affect not only the affinity for ATP, but also the interacting interface of the homodimer.[6] Therefore, it is tempting to speculate that nucleotide-binding status of FtsA could regulate its homodimerization by settling subdomain 1C in a favorable orientation for intermolecular docking.

ACKNOWLEDGMENTS

The authors thank J. Lowther for essential contribution in the production of polyclonal antibodies directed against FtsA; C. Righetti for providing purified his-MurC and for accurate technical support; F. Faggioni for invaluable sequencing work; and B. Jansson, C. Moser, N. Frandsen, S. Ferri, and M. Altieri for extensive helpful discussions. Vector pMFV12 expressing N-terminal his-FtsA was kindly provided by M.J. Ferrándiz, and the technical support in complementation assays from M. Casanova was greatly appreciated.

REFERENCES

1. van de Putte P, van Dillewijn J, Rorsch A. The selection of mutants of *Escherichia coli* with impaired cell division at elevated temperatures. Mutat Res 1964;1:121–128.
2. Rothfield L, Justice S, Garcia-Lara J. Bacterial cell division. Annu Rev Genet 1999;33:423–448.
3. Lutkenhaus J, Addinall SG. Bacterial cell division and the Z ring. Annu Rev Biochem 1997;66:93–116.
4. Addinall SG, Lutkenhaus J. FtsA is localized to the septum in an FtsZ-dependent manner. J Bacteriol 1996;178:7167–7172.
5. Wang H, Gayda RC. Quantitative determination of FtsA at different growth rates in *Escherichia coli* using monoclonal antibodies. Mol Microbiol 1992;6:2517–2524.
6. Sánchez M, Valencia A, Ferrándiz MJ, Sander C, Vicente M. Correlation between the structure and biochemical activities of FtsA, an essential cell division protein of the actin family. EMBO J 1994;13:4919–4925.
7. Dai K, Lutkenhaus J. The proper ratio of FtsZ to FtsA is required for cell division to occur in *Escherichia coli.* J Bacteriol 1992;174: 6145–6151.
8. Din N, Quardokus EM, Sackett MJ, Brun YV. Dominant C-terminal deletions of FtsZ that affect its ability to localize in Caulobacter and its interaction with FtsA. Mol Microbiol 1998;27: 1051–1063.
9. Wang X, Huang J, Mukherjee A, Cao C, Lutkenhaus J. Analysis of the interaction of FtsZ with itself, GTP and FtsA. J Bacteriol 1997;179:5551–5559.
10. Weiss DS, Chen JC, Ghigo JM, Boyd D, Beckwith J. Localization of FtsI (PBP3) to the septal ring requires its membrane anchor, the Z-ring, FtsA, FtsQ and FtsL. J Bacteriol 1999;181:508–520.
11. Ghigo JM, Weiss DS, Chen JC, Yarrow JC, Beckwith J. Localization of FtsL to the *Escherichia coli* septal ring. Mol Microbiol 1999;31:725–737.
12. Chen JC, Weiss DS, Ghigo JM, Beckwith J. Septal localisation of FtsQ, an essential cell division protein in *Escherichia coli.* J Bacteriol 1999;181:521–530.
13. Addinall SG, Cao C, Lutkenhaus J. FtsN, a late recruit to the septum in *Escherichia coli.* Mol Microbiol 1997;25:303–309.
14. Wang LL, Lutkenhaus J. FtsK is an essential cell division protein that is localized to the septum and induced as part of the SOS response. Mol Microbiol 1998;29:731–740.
15. Justice SS, García-Lara J, Rothfield LI. Cell division inhibitors SulA and MinC/MinD block septum formation at different steps in the assembly of the *Escherichia coli* division machinery. Mol Microbiol 2000;37:410–423.
16. Yim L, Vandenbussche G, Mingorance J, Rueda S, Casanova M, Ruysschaert JM, Vicente M. The role of the carboxy-terminus of *Escherichia coli* FtsA in its self-interaction and cell division. J Bacteriol 2000;182:6366–6373.
17. Feucht A, Lucet I, Yudkin MD, Errington J. Cytological and biochemical characterization of the FtsA cell division protein of *Bacillus subtilis.* Mol Microbiol 2001;40:115–125.
18. Löwe J, Amos LA. Crystal structure of the bacterial cell division protein FtsZ. Nature 1998;391:203–206.
19. van den Ent F, Löwe J. Crystal structure of the cell division protein FtsA from *Thermotoga maritima.* EMBO J 2000;19:5300–5307.
20. Nogales E, Downing KH, Amos LA, Löwe J. Tubulin and FtsZ form a distinct family of GTPases. Nat Struct Biol 1998;5:451–458.
21. Bork P, Sander C, Valencia A. An ATPase domain common to prokaryotic cell cycle proteins, sugar kinases, actin and hsp70 heat shock proteins. Proc Natl Acad Sci USA 1992;89:7290–7294.
22. Cesareni G. Peptide display on filamentous phage capsids. A new powerful tool to study protein-ligand interaction. FEBS Lett 1992;307:66–70.
23. Kay BK. Biologically displayed random peptides as reagents in mapping protein-protein interactions. Perspect Drug Discov Design 1995;2:251–268.
24. Tormo A, Martinez-Salas E, Vicente M. Involvement of the ftsA gene product in late stages of *Escherichia coli* cell cycle. J Bacteriol 1980;141:806–813.
25. Donachie WD, Begg KJ, Lutkenhaus J, Salmond GPC, Martinez-Salas E, Vicente M. Role of the ftsA gene product in control of *Escherichia coli* cell division. J Bacteriol 1979;140:338–394.
26. Guzman LM, Belin D, Carson MJ, Beckwith J. Tight regulation, modulation and high-level expression by vectors containing the arabinose P_{BAD} promoter. J Bacteriol 1995;177:4121–4130.
27. Kay BK, Winter J, McCafferty J. Phage display of peptides and proteins. San Diego CA: Academic Press; 1996. 344 p.
28. Harlow E, Lane D. Antibodies. Cold Spring Harbor, New York: Cold Spring Harbor Laboratory Press; 1988. 726 p.
29. Taylor WR. The classification of amino acid conservation. J Theor Biol 1986;119:205–218.

30. Thompson JD, Higgins DG, Gibson TJ. CLUSTALW: improving the sensitivity of progressive multiple sequence alignment through sequence weighting, position-specific gap penalties and weight matrix choice. Nucleic Acids Res 1994;22:4673–4680.
31. Altschul SF, Gish W, Miller W, Myers EW, Lipman DJ. Basic local alignment search tool. J Mol Biol 1990;215:403–410.
32. Pazos F, Olmea O, Valencia A. A graphical interface for correlated mutations and other protein structure prediction methods. Comput Appl Biosci 1997;13:319–321.
33. Vakser IA. Protein docking for low-resolution structures. Protein Eng 1995;8:371–377.
34. Pazos F, Helmer-Citterich M, Ausiello G, Valencia A. Correlated mutations contain information about protein-protein interaction. J Mol Biol 1997;271:511–523.
35. Zhou HX, Shan Y. Predictions of protein interaction sites from sequence profiles and residue neighbor list. Proteins 2001;44:336–343.
36. Fariselli P, Pazos F, Valencia A, Casadio R. Prediction of protein-protein interaction sites in heterocomplexes with neural networks. Eur J Biochem 2002;47:142–153.
37. Olmea O, Rost B, Valencia A. Effective use of sequence correlation and conservation in fold recognition. J Mol Biol 1999;295:1221–1239.
38. Holmes KC, Popp D, Gebhard W, Kabsch W. Atomic model of the actin filament. Nature 1990;347:44–49.
39. Sheterline P, Clayton J, Sparrow J. Actin. Protein Profile 1995;2:1–103.
40. Shutt CE, Myslik JC, Rozycki MD, Nalin C, Goonesekere W, Lindberg U. The structure of crystalline profilin-β-actin. Nature 1993;365:810–816.